A Tetrahedral Intermediate in the EPSP Synthase Reaction Observed by Rapid Quench Kinetics†

Karen S. Anderson,*,‡ James A. Sikorski,‡ and Kenneth A. Johnson§

Monsanto Agricultural Company, A Unit of Monsanto Company, Technology Division, 800 N. Lindbergh Boulevard, St. Louis, Missouri 63167, and Department of Molecular and Cell Biology, 301 Althouse Laboratory, The Pennsylvania State University, University Park, Pennsylvania 16802

Received November 17, 1987; Revised Manuscript Received June 9, 1988

ABSTRACT: Direct evidence for an enzyme-bound intermediate in the EPSP synthase reaction pathway has been obtained by rapid chemical quench-flow studies. The transient-state kinetic analysis has led to the following complete scheme:

$$E \underset{k_{-1}}{\overset{k_1[S3P]}{\rightleftharpoons}} E{\cdot}S3P \underset{k_{-2}}{\overset{k_2[PEP]}{\rightleftharpoons}} E{\cdot}S3P{\cdot}PEP \underset{k_{-3}}{\overset{k_3}{\rightleftharpoons}} E{\cdot}I \underset{k_{-4}}{\overset{k_4}{\rightleftharpoons}} E{\cdot}EPSP{\cdot}P_i \underset{k_{-5}[P_i]}{\overset{k_5}{\rightleftharpoons}} E{\cdot}EPSP \underset{k_{-6}[EPSP]}{\overset{k_6}{\rightleftharpoons}} E$$

Values for all 12 rate constants were obtained. Substrate trapping experiments in the forward and reverse reactions established the kinetically preferred order of binding and release of substrates and products and showed that shikimate 3-phosphate (S3P) and 5-enolpyruvoylshikimate 3-phosphate (EPSP) dissociate at rates greater than turnover in each direction. Pre-steady-state bursts of product formation were observed in the reaction in each direction indicating a rate-limiting step following catalysis. Single turnover experiments with enzyme in excess over substrate demonstrated the formation of a transient intermediate in both the forward and reverse reactions. In these experiments, the enzymatic reaction was observed by employing a radiolabel in the enol moiety of either phosphoenol pyruvate (PEP) or EPSP. The separation and quantitation of reaction products were accomplished by HPLC monitoring radioactivity. The intermediate was observed as the transient production of radiolabeled pyruvate, formed due to the breakdown of the intermediate in the acid quench used to stop the reaction. The intermediate was observed within 5–10 ms after the substrates were mixed with enzyme and decayed in a reaction paralleling the formation of product in each direction. Thus, the kinetics demonstrate directly the kinetic competence of the presumed intermediate. No pyruvate was formed, on a time scale which is relevant to catalysis, after incubation of the enzyme with dideoxy-S3P and PEP or with EPSP in the absence of phosphate; and so, the intermediate does not accumulate under these conditions. The intermediate broke down to form PEP and EPSP in addition to pyruvate when the reaction was quenched with base rather than acid; therefore, the intermediate must contain the elements of each product. Other experiments were designed to measure directly the phosphate binding rate and further constrain the PEP binding rate. The overall solution equilibrium constant in the forward direction was determined to be 180 by quantitation of radiolabeled reactants and products in equilibrium after incubation with a low enzyme concentration. The internal, active site equlibrium constant was obtained by incubation of radiolabeled S3P with excess enzyme and high concentrations of phosphate and PEP to provide the ratio of [EPSP]/[S3P] = 2.3, which is largely a measure of K_4. These values, in addition to the equilibrium constants for S3P and EPSP binding and the steady-state kinetic parameters, allow us to provide estimates for all of the rate constants describing the reaction pathway as the best fit to all of the pre-steady-state kinetics by computer simulation. The kinetics are indicative of a single intermediate in the reaction sequence and provide no support for multiple intermediates along the reaction pathway. The data suggest an addition–elimination reaction proceeding via a tetrahedral intermediate formed by the nucleophilic attack of the 5-OH of S3P on C-2 of PEP.

EPSP (5-enolpyruvoylshikimate 3-phosphate)[1] synthase catalyzes the transfer of an enolpyruvoyl moiety from phosphoenolpyruvate (PEP) to shikimic acid 3-phosphate (S3P). The enzyme is inhibited by the commercially important herbicide glyphosate, which competes with PEP in binding to the enzyme in the presence of S3P (Steinrucken & Amrhein, 1980). Although it has been suggested that glyphosate mimics the transition state for the reaction, the mechanism of the EPSP synthase has not been established. Knowledge of the enzyme reaction pathway is important in understanding the inhibition by glyphosate of this unique enzymatic reaction.

Only one other enzyme is known to catalyze the transfer of an enolpyruvoyl moiety from phosphoenolpyruvate; UDP-*N*-acetylglucosamine enolpyruvoyl transferase catalyzes the first committed step in biosynthesis of bacterial cell wall peptidoglycan by transferring the enolpyruvate moiety of PEP to the oxygen attached to C-3 of the glucosamine moiety of UDP-*N*-acetylglucosamine. This enzyme is not inhibited by glyphosate. Evidence has been obtained suggesting the

† K.A.J. was supported by an Established Investigatorship from the American Heart Association with funds contributed in part by the Pennsylvania Affiliate. This work was supported in part by NIH Grant GM26726 to K.A.J.

* Author to whom correspondence should be addressed.
‡ Monsanto Agricultural Co.
§ The Pennsylvania State University.

[1] Abbreviations: dideoxy-S3P, 4,5-dideoxyshikimic acid 3-phosphate; EPSP, 5-enolpyruvoylshikimate 3-phosphate; glyphosate, *N*-(phosphonomethyl)glycine; HEPES, *N*-(2-hydroxyethyl)piperazine-*N*′-2-ethanesulfonic acid; S3P, shikimate 3-phosphate; PEP, phosphoenol pyruvate; P_i, inorganic phosphate.

0006-2960/88/0427-7395$01.50/0

Scheme I

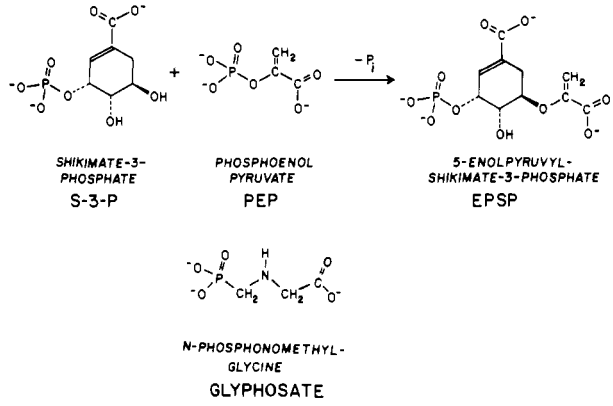

presence of a covalent enolpyruvoyl–enzyme intermediate in the reaction pathway (Zemell & Anwar, 1975). On the basis of this precedent, there have been several attempts to obtain evidence for an enzyme–enolpyruvoyl intermediate with EPSP synthase.

The reaction catalyzed by EPSP synthase and the chemical structure of glyphosate are shown in Scheme I. The first mechanistic study on the enzyme by Bondinell et al. (1971) showed that the reaction proceeds with C–O cleavage of the phosphate ester. In addition, studies of the reaction in D_2O and in ^3H_2O provided evidence for exchange of the methylene protons on C-3 of PEP. These data were taken to suggest an enzyme reaction mechanism proceeding through a tetrahedral intermediate formed by the nucleophilic attack of the 5-OH of S3P on C-2 of PEP but are consistent with other mechanisms as well. Grimshaw et al. (1982) confirmed and extended these studies to show a primary deuterium isotope effect involving the C-3 of PEP wherein there was a substantial discrimination against heavy hydrogen in both the protonation and deprotonation steps, thus providing further support for a direct addition–elimination reaction mechanism. However, subsequent work by Anton et al. (1983) further showed that the enzyme catalyzes the exchange of ^3H from solvent into PEP in the presence of dideoxy-S3P, a substrate analogue lacking the hydroxyl groups. Although the rate of exchange observed in this study was much slower than catalytic turnover, these authors concluded that the enzyme proceeded via an enzyme–enolpyruvoyl intermediate which could be formed in the absence of the 5-OH of S3P.

In spite of several proposed enzyme intermediates in the EPSP synthase reaction pathway, there has been no direct demonstration of any intermediate. In this paper we describe rapid chemical quench-flow data, providing a direct demonstration and complete kinetic characterization of an intermediate in the reaction pathway. The data are most consistent with a simple addition–elimination reaction proceeding via a tetrahedral intermediate.

Materials and Methods

Enzyme Purification. EPSP synthase was isolated from a cloned *Escherichia coli* strain which overproduces the enzyme (Rogers et al., 1983). The purification procedure employed is outlined as follows: (1) protamine sulfate precipitation to remove nucleic acid as described by Pittard et al. (1979); (2) ammonium sulfate fractionation (50–70%); (3) phenyl-Sepharose CL-4B chromatography with elution using a linear gradient of 0.8–0.0 M ammonium sulfate in 25 mM Tris-HCl, pH 7.5; (4) Mono-Q chromatography (HR 10/10 column, Pharmacia) using a 30-min linear gradient of 0–300 mM KCl in 25 mM Tris-HCl, pH 7.5. The specific activity of the final protein solution after concentration was 70 μmol min^{-1} mg^{-1} as determined by assaying the release of inorganic phosphate by the method of Lanzetta et al. (1979). The enzyme concentration was determined with an extinction coefficient of 0.77 cm^2/mg at 280 nm.

Chemicals. Shikimate 3-phosphate (S3P) was synthesized enzymatically by treatment of shikimic acid (Sigma Chemical Co.) with shikimate kinase (Millar et al., 1986). S3P was purified by chromatography on DEAE-Sephadex A-25 eluted with a gradient of triethylammonium bicarbonate. The sodium salt of S3P was obtained by passing it through a Dowex-50 column (Na^+ form). The S3P was standardized by NMR with 1-methyl-1*H*-1,2,4-triazole as an internal standard. In the NMR standardization method, preweighed samples of 1-methyltriazole and S3P were diluted with D_2O so the concentration of methyltriazole was known. A spectrum of this mixture was then taken, and the area for the proton in the 5-position of the triazole appearing at 8.0 ppm was compared with the area for the vinyl shikimate ring proton for S3P which appeared at 7.2 ppm.

[^{14}C]S3P was synthesized and purified in a similar manner, starting with uniformly labeled shikimic acid (New England Nuclear, Boston, MA). The specific activity of the [^{14}C]-shikimic acid was 19 mCi/mmol.

EPSP was synthesized enzymatically from S3P and PEP (Sigma Chemical Co.), with EPSP synthase. Purification and standardization was accomplished in a manner similar to that described for S3P. The [^{14}C]EPSP was prepared in a similar manner with radiolabeled S3P or radiolabeled [^{14}C]PEP (New England Nuclear, sp act. 32 mCi/mmol). In some cases doubly labeled EPSP was used which was prepared enzymatically from the radiolabeled S3P and PEP.

All buffers and other reagents employed were of highest commercial purity. Millipore ultrapure water was used for all solutions. All experiments were conducted at 20 °C in HEPES buffer (50 mM) containing potassium chloride (50 mM) at pH 7.0.

Rapid Quench Experiments. The rapid quench experiments were performed in an apparatus designed and built by Johnson (1986). The reaction was initiated by mixing the enzyme solution (45 μL) with the radiolabeled substrates (45 μL). In all cases, the concentrations of enzyme and substrates cited in the text are those after mixing and during the enzymatic reaction. The reaction mixture was then quenched by mixing with 45 μL of 0.6 N HCl to give a final concentration of 0.2 N HCl. The quenched reaction solution was collected in a 1.5-mL Eppendorf tube containing chloroform (100 μL), vortexed, and then neutralized by the addition of an aliquot of 4 N KOH in 1 M Tris. The chloroform was included to irreversibly denature the enzyme and allow removal of the protein before analysis by HPLC; without chloroform treatment, some enzyme activity was regained upon neutralization of the acid. The substrate and products were quantitated by HPLC as described below. In order to ensure that the acid was quenching the enzymatic reaction, a control was included with each experiment. This involved adding the enzyme to a premixed solution of acid and substrates. Control experiments were also done to establish the stability of the radiolabeled substrates under the quench conditions employed.

HPLC Analysis. The substrates and products were quantitated by HPLC with a radioactivity detector. The HPLC separation was performed on a Mono-Q anion-exchange column (HR 5/5, Pharmacia, Piscataway, NJ) with a flow rate of 2 mL/min. The following gradient separation was employed where solvent A is ultrapure water and solvent B

is 0.5 M ammonium bicarbonate. The linear gradient program was as follows: 35–70% B in 5 min, hold at 70% B for 4 min, recycle to 35% B in 3 min, and reequilibrate at 35% B for 6 min. The HPLC effluent from the column was then mixed with liquid scintillation cocktail (Atomlight, New England Nuclear) with a flow rate of 6 mL/min. Radioactivity was monitored continuously with a Flo-One radioactivity detector (Radiomatic Instruments, Tampa, FL). The analysis system was automated by the use of a Waters WISP (Milford, MA) autosampler.

Substrate Trapping Experiments. The amount of S3P, PEP, or EPSP which could be trapped at the active site of the enzyme was determined by mixing a solution of enzyme and radiolabeled substrate with a solution containing an excess of unlabeled substrate (>35-fold excess) and the cosubstrate necessary for catalysis. The concentration of the enzyme–substrate complex in the preincubation mixture was calculated according to the quadratic equation using the concentrations of enzyme and substrate in the syringe before mixing and then corrected for the 2-fold dilution during mixing. All concentrations cited throughout the text are those during the enzymatic reaction after mixing.

In conducting the EPSP trapping experiment, it was found that EPSP was hydrolyzed at a very slow rate in an enzyme-catalyzed reaction occurring in the absence of phosphate.[2] The rate of hydrolysis was measured by following the time dependence of conversion of enol-labeled EPSP to pyruvate. The reaction was followed under conditions of enzyme in excess over the substrate, and accordingly, the observed rate provided a direct measurement of the rate constant for hydrolysis at the active site as a first-order process (4.7×10^{-4} s^{-1}). The EPSP trapping experiment was completed within one half-life of the hydrolysis reaction (24 min) after enzyme was mixed with substrate, and the data were corrected for the extent of hydrolysis according to the time that each sample was collected.

Equilibrium Measurements. Experiments were conducted to determine both the internal (enzyme bound) and the overall (solution) equilibrium constants. The solution equlibrium constant was determined by mixing a low concentration of enzyme (0.10 μM), doubly labeled [^{14}C]EPSP (4 μM), and phosphate (1 mM) and allowing the solution to come to equlibrium (~3 h); the solution was quenched with acid and chloroform as described above. The relative amounts of [^{14}C]S3P, [^{14}C]PEP and [^{14}C]EPSP were then determined by HPLC as described above. The equilibrium constant was calculated from K = [EPSP][P_i]/[S3P][PEP].

The internal equilibrium constant was determined by mixing a high concentration of enzyme (16 μM) with [^{14}C]S3P (4 μM), PEP (2 mM), and phosphate (10 mM). The mixture was incubated for 15 s and then quenched by acid as described above. The relative amounts of S3P and EPSP were then determined by HPLC.

All equilibrium constants are calculated for the reaction in the forward direction according to Scheme II.

Fluorescence Titration Measurements. Equilibrium fluorescence measurements were made in a manner as described previously (Anderson et al., 1988a). The dissociation constant for dideoxy-S3P was determined by competition versus EPSP where the apparent K_d value for EPSP was measured in the presence of a fixed concentration of dideoxy-S3P (1 mM). Under these conditions the apparent dissociation constant for EPSP is equal to $K^{app}_{EPSP} = K_{d,EPSP}$ (1 + $[S_0]/K_{d,S}$), where S represents dideoxy-S3P, and $K_{d,EPSP}$ and $K_{d,S}$ and the true dissociation constants for EPSP and dideoxy-S3P, respectively. Solving this expression for $K_{d,S}$ provided a dissociation constant of 100 μM for dideoxy-S3P binding to the enzyme.

A fluorescence change was observed when PEP bound to the preformed enzyme–dideoxy-S3P complex; this fluorescence change was titrated to provide a direct measurement of the dissociation constant (23 μM) for PEP binding to the enzyme–dideoxy-S3P complex.

Data Analysis. The KINSIM kinetic simulation program (kindly provided by Carl Frieden and Bruce Barshop, Washington University, St. Louis, MO; Barshop et al., 1983) was used to model all of the kinetic data presented in this paper. The program was modified to allow the input of data from the rapid quench experiments as x,y pairs and to calculate the sum square errors in fitting the data.

The availability of software for the simulation of enzyme kinetics sets a new standard in the fitting of pre-steady-state kinetic data. It is no longer adequate to extract constants by fitting simplified models to experiments performed under different sets of conditions. Rather, the entire data set can now be fit to a single model and a single set of rate constants. The goal then is to sufficiently constrain the various rate constants to find a single minimum in fitting the data. This has been achieved for the current data.

The data were fit by a trial and error process maintaining the constraints of the known dissociation constants for S3P and EPSP (Anderson et al., 1988a), the K_m values for PEP and P_i (Duncan et al., 1984), and by the overall equilibrium constant, $K_1K_2K_3K_4K_5K_6 = 180$, and the internal equilibrium constant, $K_{int} = 2.3$, measured as described under Results. These constraints allowed for only one best fit to the data. The final refinement in fitting the data was achieved by minimizing the sum square error with respect to each constant while holding the remaining constants fixed at their best value. Of course only a subset of the 12 constants were important determinants in fitting the data for each experiment, while other constants were held fixed at the values specified by other experiments. In particular, the S3P and EPSP off rates were obtained by fitting the trapping experiments, and because the values were faster than other constants, variations in their values over a wide range had little effect on the fits to the other pre-steady-state data; accordingly, the values determined by fitting the trapping experiments were held fixed in fitting other data. The binding rates for S3P and EPSP were calculated from the dissociation constants and the dissociation rates. The rate of phosphate binding was determined by the fit to the data in Figure 4 with all other constants fixed at their best values, and then this rate was not varied in refining the fits to other data. The PEP binding rate was estimated from the S3P trapping reaction as described under Results. The remaining constants, k_{-2}, k_3, k_{-3}, k_4, k_{-4}, and k_5 were obtained as the best fit to all of the kinetic data, in particular the experiments described in Figures 7 and 8, and the internal equilibrium data. The rate of appearance of the intermediate in the forward reaction (Figure 7) required the relatively fast rate for k_3. The values of k_4 and k_{-4} were determined by the amplitude of the transient appearance of the intermediate in both the forward and reverse directions. The net rates of turnover in the forward and reverse directions then established the values of k_5 and k_{-3}, respectively.

RESULTS

Preface. The rapid kinetic analysis described in this paper leads to kinetic Scheme II, where E·I represents an enzyme-

[2] Dr. R. D. Sammons, personal communication.

Table I: Distribution of Products Formed in Acid or Base[a]

quench	pyruvate (μM)	PEP (μM)	EPSP (μM)
acid	1.24	0.57	1.69
base	0.33	0.96	2.21
base − acid	−0.91	0.39	0.52
% yield	27	31	42

[a] A solution containing EPSP synthase (40 μM) and S3P (100 μM) was mixed with [^{14}C]PEP (3.5 μM), and the reaction was then quenched after 10 ms by mixing with either 0.2 N HCl or 0.2 N KOH (all concentrations are those after mixing). The distribution of label appearing in pyruvate, PEP, or EPSP is given in units of concentration during the enzymatic reaction. The percent yield was calculated from the fraction of the pyruvate seen in the acid quench partitioning into each species in the base quench. Conditions: 50 mM HEPES, 50 mM KCl, pH 7.0, and 20 °C.

bound intermediate. The kinetics are in some instances quite complex because they are a function of many of the 12 rate constants. Nonetheless, the experiments described in the paper allow us to define a single set of rate constants that account for all the data. Each kinetic experiment has been simulated by numerical integration using one set of rate constants (see Table II) with no simplifying assumptions, and the results of these simulations are presented with each figure. Because many of the results are difficult to understand by themselves and because we wish to present a unified model for all of the kinetic data, reference to this scheme will be made throughout the presentation of the results. In particular, the extent to which each result defines a portion the the reaction pathway will be clarified by reference to Scheme II.

Scheme II

$$E \underset{k_{-1}}{\overset{k_1[S3P]}{\rightleftharpoons}} E{\cdot}S3P \underset{k_{-2}}{\overset{k_2[PEP]}{\rightleftharpoons}} E{\cdot}S3P{\cdot}PEP \underset{k_{-3}}{\overset{k_3}{\rightleftharpoons}} E{\cdot}I \underset{k_{-4}}{\overset{k_4}{\rightleftharpoons}}$$
$$E{\cdot}EPSP{\cdot}P_i \underset{k_{-5}[P_i]}{\overset{k_5}{\rightleftharpoons}} E{\cdot}EPSP \underset{k_{-6}[EPSP]}{\overset{k_6}{\rightleftharpoons}} E$$

S3P Trapping Experiments. We began our studies to establish the EPSP synthase pathway by investigating the order of substrate binding in the forward and reverse reactions. Previously reported experiments have suggested that S3P binds first followed by PEP (Boocock & Coggins, 1983) although others have suggested a random mechanism (Streinrucken & Amrhein, 1984).

In an S3P trapping experiment, radiolabeled substrate, [^{14}C]S3P was premixed with enzyme, and then the enzymatic reaction was initiated by the addition of PEP and an excess of unlabeled S3P. If the PEP can react with the preformed E·S3P complex, then radiolabeled EPSP will be formed in a single turnover. The amount of radiolabeled EPSP will be a function of the kinetic partitioning established by the rate of

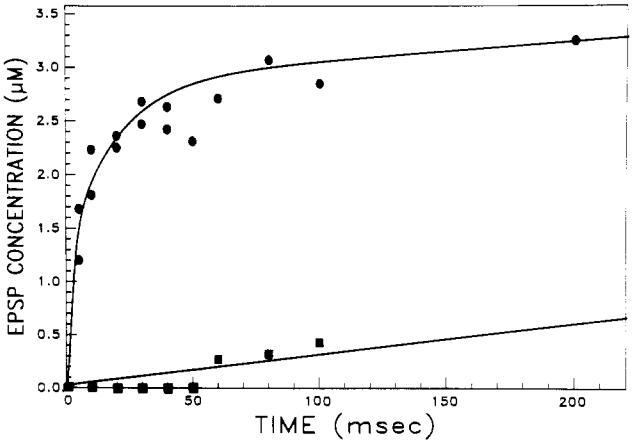

FIGURE 1: Time course of turnover of S3P trapped at the enzyme active site. A solution containing [^{14}C]S3P (25 μM) and enzyme (5 μM) was mixed with a solution of unlabeled S3P (1.75 mM) and PEP (1 mM) (final concentrations); after various times, the reaction was stopped by the addition of 0.2 N HCl, and the formation of radiolabeled EPSP was quantified by HPLC as described under Materials and Methods (●). In a parallel experiment, we attempted to trap PEP at the enzyme active site. A solution containing [^{14}C]PEP (25 μM) and enzyme (5 μM) was mixed with a solution of unlabeled PEP (1.75 mM) and S3P (1 mM) (final concentrations), and the formation of radiolabeled EPSP was monitored as above (■). Each curve was calculated by computer simulation of the kinetics with the rate constants summarized in Table II. Simulation of the PEP trapping experiment assumed that the rate of EPSP production was due to turnover of radiolabeled PEP diluted into the unlabeled pool.

PEP binding and the rate of dissociation of E·S3P complex according to the pathway:

$$E \cdot S3P^* \underset{k_{-2}}{\overset{k_2}{\rightleftharpoons}} E \cdot S3P^* \cdot PEP \xrightarrow{k_3} E + EPSP^* + P_i$$
$$k_{-1} \downarrow$$
$$E + S3P^*$$

Analysis of the PEP concentration dependence of the trapping reaction can also provide estimates of the rate of dissociation of the radiolabeled S3P (k_{-1}) and the rate of binding of PEP (k_2).

A time course of trapping S3P at the enzyme active site was determined by mixing a solution of [^{14}C]S3P (25 μM) and enzyme (5 μM) with high concentrations of unlabeled S3P (1.75 mM) and PEP (1 mM). In all cases, the concentrations of enzyme and substrates cited in the text are those after mixing and during the enzymatic reaction. At various times after mixing, the reaction was quenched by mixing with HCl, and the amount of radiolabeled EPSP was determined by HPLC as described under Materials and Methods. The time-dependent formation of radiolabeled EPSP is shown in Figure 1 (circles). The data show a rapid rise followed by a

Table II: EPSP Synthase Kinetic Constants[a]

$$E \underset{k_{-1}}{\overset{k_1}{\rightleftharpoons}} E{\cdot}S3P \underset{k_{-2}}{\overset{k_2}{\rightleftharpoons}} E{\cdot}S3P{\cdot}PEP \underset{k_{-3}}{\overset{k_3}{\rightleftharpoons}} E{\cdot}I \underset{k_{-4}}{\overset{k_4}{\rightleftharpoons}} E{\cdot}EPSP{\cdot}P_i \underset{k_{-5}}{\overset{k_5}{\rightleftharpoons}} E{\cdot}EPSP \underset{k_{-6}}{\overset{k_6}{\rightleftharpoons}} E$$

step	reaction	k_+	k_-	K_{eq}
1	E + S3P ⇌ E·S3P	650 μM^{-1} s^{-1}	4500 s^{-1}	0.14 μM^{-1}
2	E·S3P + PEP ⇌ E·S3P·PEP	15 μM^{-1} s^{-1}	280 s^{-1}	0.054 μM^{-1}
3	E·S3P·PEP ⇌ E·I	1200 s^{-1}	100 s^{-1}	12
4	E·I ⇌ E·EPSP·P_i	320 s^{-1}	240 s^{-1}	1.4
5	E·EPSP·P_i ⇌ E·EPSP + P_i	100 s^{-1}	0.07 μM^{-1} s^{-1}	1430 μM
6	E·EPSP ⇌ E + EPSP	200 s^{-1}	200 μM^{-1} s^{-1}	1 μM
	S3P + PEP ⇌ EPSP + P_i			180
	E·S3P + P_i ⇌ E·S3P·P_i	1.5 μM^{-1} s^{-1}	1000 s^{-1}	0.0015 μM^{-1}
	E·EPSP → E·S3P·pyruvate	0.00047 s^{-1}		

[a] These kinetic constants represent the best fit for all of the kinetic and equilibrium data given in this paper. Equilibrium constants and free energies were calculated for the forward reaction as written. The overall equilibrium constant in solution is given by the product $K_1K_2K_3K_4K_5K_6$ = 180, for the forward reaction. Conditions: 50 mM HEPES, 50 mM KCl, pH 7.0, and 20 °C.

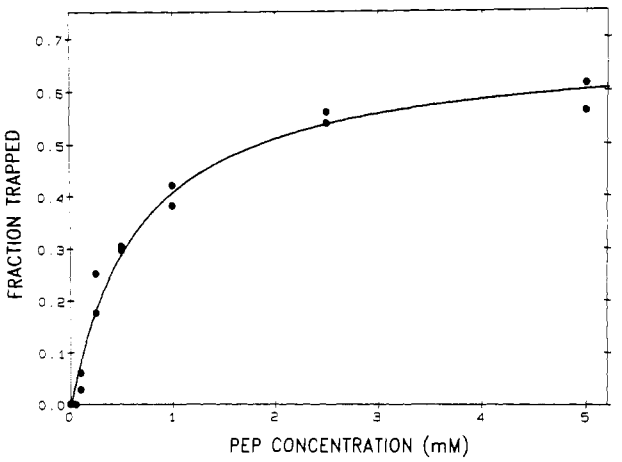

FIGURE 2: PEP concentration dependence of the S3P trapped. The fraction of S3P trapped at the active site was determined at various concentrations of PEP. A solution of enzyme (10 μM) and [^{14}C]S3P (5.5 μM) was mixed with a solution containing unlabeled S3P (1 mM) and varying concentrations of PEP (10–5000 μM), final concentrations. The reaction mixture was quenched by the addition of 0.2 N HCl after 200 ms, and the amount of [^{14}C]EPSP (●) was determined by HPLC as described under Materials and Methods. The curve was obtained by fitting the data to a hyperbola by nonlinear regression to give the maximum trapped as 70 ± 3% and the concentration of PEP required for half-maximal trapping as 640 ± 70 μM.

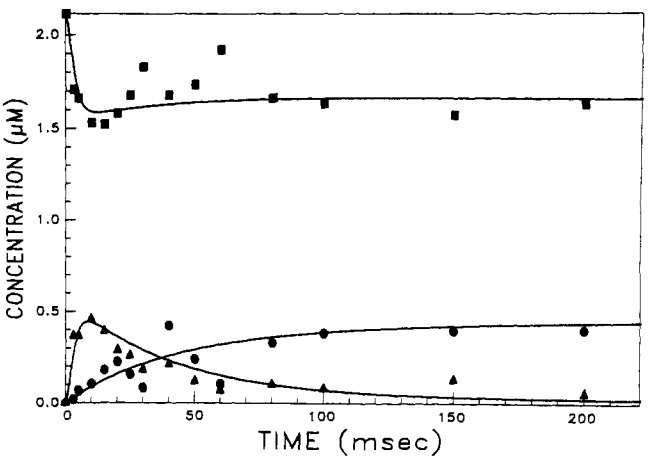

FIGURE 3: A time course of turnover of EPSP trapped at the enzyme active site. A solution of [^{14}C]EPSP and enzyme was mixed with a solution of cold EPSP and phosphate. The final concentrations were [^{14}C]EPSP (2 μM), enzyme (10 μM), cold EPSP (500 μM), and phosphate (7.5 mM). The concentrations of radiolabeled EPSP (■), pyruvate (▲), and PEP (●) were determined by HPLC. The curves were calculated by computer simulation with the constants summarized in Table II.

slower linear phase. The amplitude of the reaction corresponds to 72% of the E·S3P* trapped. This result demonstrates that the enzymatic reaction can proceed in the order with S3P binding first, followed by PEP.

The converse experiment, to determine the amount of PEP which can be trapped, involved mixing [^{14}C]PEP (25 μM) and enzyme (5 μM) with high concentrations of unlabeled PEP (1.75 mM) and S3P (1 mM). In this case the small amount of EPSP produced could be accounted for by the rate of turnover of the radiolabeled PEP after dilution into the unlabeled pool as shown in Figure 1 (squares). These data indicate that PEP does not bind to enzyme in the absence of S3P in a mode kinetically competent to carry out catalysis. The combination of these two trapping experiments establishes the kinetically preferred order of the enzymatic reaction as S3P binding first followed by PEP binding second as shown in Scheme II.

In order to gain more quantitative information on the kinetic partitioning between dissociation of S3P and the binding of PEP, it was necessary to estabish the PEP concentration required for half-maximal trapping of the S3P. The amplitude of the trapping reaction was measured after 200 ms of reaction with various concentrations of PEP to provide the results shown in Figure 2. The fraction of the radiolabeled S3P trapped increased hyperbolically to a maximum equal to 72% of the E·S3P* present at the start of the reaction (calculated from the previously measured dissociation constant, $K_{d,S3P}$ = 8 μM; Anderson et al., 1988a). The PEP concentration at which half of the maximum S3P becomes trapped, $K_{t,PEP} \simeq 600$ μM, was obtained by fitting the data in Figure 2 to a hyperbola. According to the partition analysis described by Rose (1980), one can estimate that the rate of S3P dissociation, k_{-1}, lies between the limits

$$k_{cat}\frac{K_{t,PEP}}{K_{m,PEP}} < k_{-1} > k_{cat}\frac{K_{t,PEP}}{K_{m,PEP}}\frac{[E\cdot S3P^*]_0}{P^*_\infty}$$

where $K_{m,PEP}$ is the Michaelis constant for PEP (12–16 μM) and $P^*_\infty/[E\cdot S3P^*]_0$ is the fraction of S3P trapped at saturating PEP concentration (Rose, 1980). With a turnover number of k_{cat} = 60 s^{-1}, these data constrain the rate of S3P dissociation to lie within the range of 2200–4500 s^{-1}. Combined with the equilibrium constant for S3P ($K_{d,S3P}$ = 8 μM), this predicts a binding rate constant of (3–6) × 10^8 M^{-1} s^{-1}.

The S3P trapping data also provide an estimate for the magnitude of k_2, the rate of PEP binding according to (Rose, 1980)

$$K_{t,PEP} = \frac{k_{-1}}{k_2}\left(\frac{k_{-2} + k_3}{k_3}\right)$$

when the rate of dissociation of S3P from the E·S3P·PEP complex is negligible (see below). Given the allowable range in the ratio of $(k_{-2} + k_3)/k_3$ determined by the transient kinetic data described below, the value of k_2 is constrained to lie in the range of 5–15 μM^{-1} s^{-1}.

EPSP Trapping Experiments. The order of substrate binding in the reverse direction was examined by determining the amount of EPSP which could be trapped by mixing with phosphate. A time course of trapping EPSP at the active site was determined by mixing a solution of [^{14}C]EPSP (2.0 μM) and enzyme (10 μM) with a solution of unlabeled EPSP (500 μM) and phosphate (7.5 mM). The experiment was conducted with the enzyme in excess over substrate to obtain a higher amplitude and thus a better signal for the amount of EPSP trapped as radiolabeled PEP. This experiment was difficult to perform because it was found that in the absence of phosphate the enzyme hydrolyzes EPSP to S3P and pyruvate at a slow rate (4.7 × 10^{-4} s^{-1}). In order to overcome this complication, the experiment was completed in less than one half-life of the hyrolysis reaction after mixing enzyme with EPSP (24 min), and the data were corrected for this slow rate of hydrolysis occurring during the time required to perform the experiment.

The time course of PEP formation after a preformed E·EPSP complex was mixed with the trapping solution is shown in Figure 3. At long times, there was a net conversion of ~20% of the bound [^{14}C]EPSP into PEP. However, the kinetics of the reaction were complex with a transient appearance and disappearance of [^{14}C]pyruvate and a corresponding transient change in the concentration of EPSP peaking at 10 ms. Control experiments in the absence of enzyme established that pyruvate was not a breakdown product of PEP or EPSP with the quenching conditions employed.

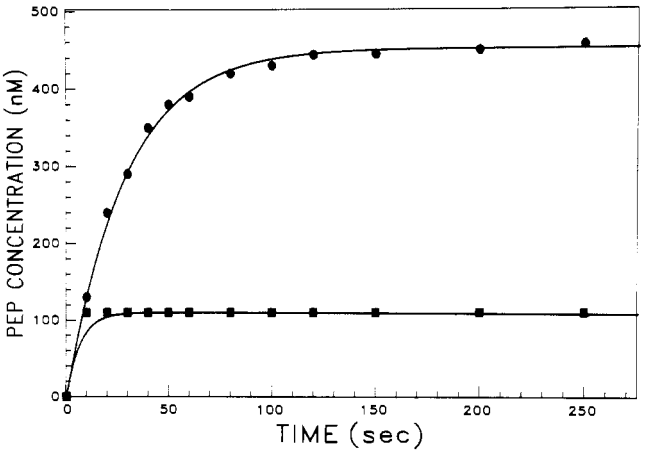

FIGURE 4: Rate of phosphate binding. A solution of 5 μM enzyme was mixed with 1 mM EPSP and 0.5 μM [^{32}P]phosphate. At various times after mixing, the reaction was quenched by the manual addition of 0.2 N HCl, and the concentrations of [^{32}P]phosphate and [^{32}P]PEP were determined by HPLC. The reaction was run with (●) or without (■) the addition of 2 mM unlabeled PEP. The curves were simulated with the constants summarized in Table II and as described in the text.

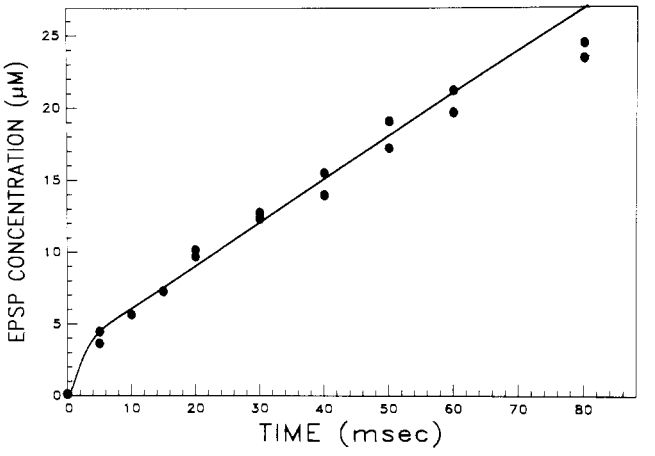

FIGURE 5: Kinetics of a pre-steady-state burst in the forward reaction. A solution of enzyme and [^{14}C]S3P was mixed with a solution of PEP to give a final concentrations of S3P (50 μM), enzyme (10 μM), and PEP (1 mM). The formation of radiolabeled EPSP was monitored (●). The curve represents the prediction by kinetic simulation with the rate constants listed in Table II.

Moreover, the enzyme does not catalyze the hydrolysis of PEP, and the enzyme-catalyzed hydrolysis of EPSP (described above) could not account for the transient changes observed. As described below, the production of pyruvate and the transient change in the concentration of EPSP is due to the formation of an enzyme-bound intermediate which breaks down to pyruvate in the acid quench. The rate of breakdown of the intermediate to produce PEP in the reverse direction is slow relative to steps in the forward reaction leading toward the release of EPSP and phosphate, thus accounting for the transient rise and fall in concentrations of pyruvate (intermediate) and EPSP bound to the enzyme site. On the basis of the kinetic parameters established below, the curves shown in Figure 3 were calculated under conditions to simulate the EPSP trapping experiment with the constants summarized in Table II. The EPSP trapping experiment served to define only the rate of EPSP dissociation, k_6 = 200 s^{-1}, using the rate of phosphate binding measured below.

In spite of complications in the kinetics of the trapping reaction, this experiment demonstrates that EPSP could be trapped at the active site, supporting an ordered mechanism with EPSP binding first in the reverse reaction. A converse experiment, to examine if phosphate could be trapped at the active site, was not feasible due to weak phosphate binding (K_m = 2.5 mM). However, in the experiments performed to measure the internal chemical equilibrium at the active site of the enzyme (see below), it was shown that a high concentration of phosphate could lock EPSP onto the enzyme. Therefore, the order of product release must be P_i first followed by EPSP as described in Scheme II.

Measurement of the Phosphate Binding Rate. Quantitative interpretation of the EPSP trapping experiments required an independent estimate of the rate of phosphate binding. Accordingly, an experiment was conducted under conditions where the rate of phosphate binding would limit the rate of PEP formation from EPSP. A solution of enzyme (5 μM) was mixed with a solution of EPSP (1 mM) and [^{32}P]phosphate (0.5 μM) (final concentrations). The time course for the formation of [^{32}P]PEP was then measured (Figure 4). The experiment was conducted over a period of 300 s in the absence (squares) and presence (circles) of 2 mM unlabeled PEP. It was surprising that the reaction appeared to reach a plateau (~20% completion) within 10 s (the first reaction time point) in the absence of added unlabeled PEP. The data indicate that the reaction came to equilibrium even though the high concentration of EPSP would be expected to drive the reverse reaction to completion. However, when the experiment was conducted in the presence of a high concentration of unlabeled PEP (circles), the radiolabeled PEP was chased off of the enzyme, and the reaction went to completion. In the latter case, the kinetics are simple to interpret and provide a direct measurement of the rate of phosphate binding, best fit by a value of 0.06–0.07 μM^{-1} s^{-1}.

A quantitative explanation for the reaction performed in the absence of added PEP can be obtained if we considered the amount of S3P which could be produced by the slow hydrolysis of EPSP and the amount which might be present in the EPSP as a contaminant. Allowing for only ~1.5% of the EPSP to break down to S3P provides a sufficient concentration, and the reaction is predicted to come to equilibrium with most of the observed PEP in solution and with a small but significant fraction bound to the enzyme in the E·S3P·PEP complex. The curves drawn in Figure 4 were simulated according to these conditions (see Discussion), confirming our interpretation quantitatively with no simplifying assumptions. This interpretation implies that the internal equilibrium on the enzyme favors the products EPSP and phosphate. This is confirmed by the measurements described below.

A Pre-Steady-State Burst of Product Formation. Knowing the orders of product binding and substrate release, we began our efforts to explore the events occurring at the active site by performing a rapid chemical quench-flow experiment to look for a pre-steady-state burst of product formation. The time course for the forward reaction was determined by mixing a solution containing enzyme and [^{14}C]S3P (premixed) with a solution containing an excess of PEP to initiate the reaction. The final concentrations after mixing were 10 μM enzyme, 50 μM [^{14}C]S3P, and 1 mM PEP. At various times after mixing the reaction was quenched by the addition of 0.2 N HCl (final concentration). The quenched reaction mixture was then neutralized, and the amount of radiolabeled EPSP was quantitated by HPLC as described under Materials and Methods. The time-dependent formation of radiolabeled EPSP is shown in Figure 5. A pre-steady-state burst with an amplitude of 0.3 per enzyme site and a rate in excess of 250 s^{-1} was observed. These data indicate that a step occurring after catalysis was at least partially rate limiting.

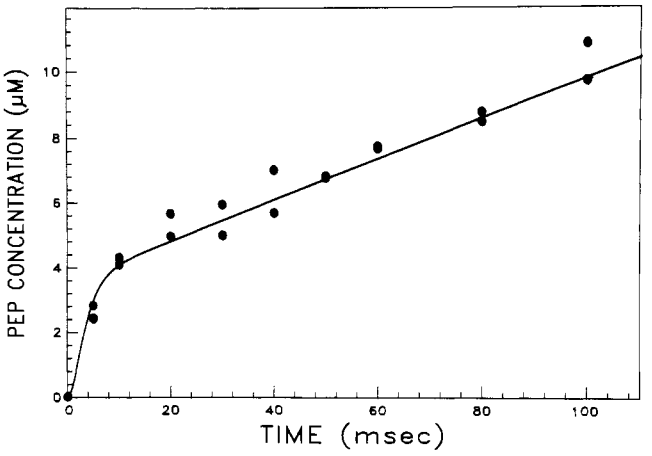

FIGURE 6: Kinetics of a pre-steady-state burst in the reverse reaction. A solution of enzyme was mixed with a solution of [^{14}C]EPSP (enol labeled) and phosphate to give final concentrations of enzyme (10 μM), EPSP (50 μM), and phosphate (7.5 mM). The formation of radiolabeled PEP was monitored (●). The curve was calculated by computer simulation with the constants summarized in Table II.

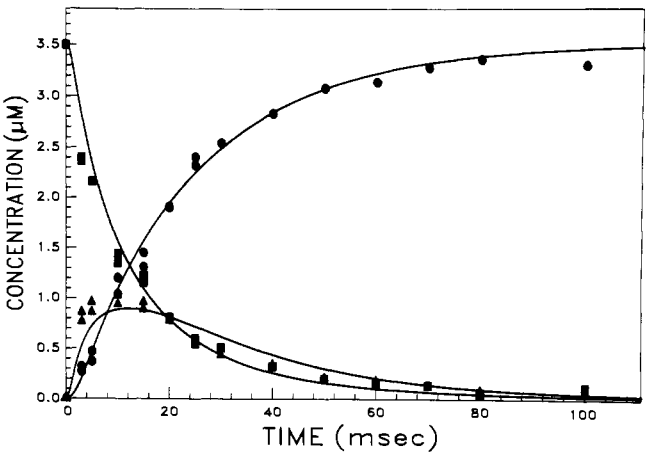

FIGURE 7: A single turnover in the forward reaction. A solution of S3P and enzyme was mixed with a solution of [^{14}C]PEP to initiate the reaction. The final concentrations were S3P (100 μM), enzyme (10 μM), and [^{14}C]PEP (3.5 μM). The formation and disappearance of pyruvate (▲), PEP (■), and EPSP (●) were monitored. The curves were calculated by numerical integration with the rate constants summarized in Table II.

A similar experiment was performed to examine the rate-limiting step in the reverse direction. The reaction was begun by mixing a solution of enzyme (10 μM) with a solution containing [^{14}C]EPSP (50 μM) and phosphate (7.5 mM). The time-dependent formation of radiolabeled PEP is shown in Figure 6. A pre-steady-state burst with an amplitude of 0.4 per enzyme site and a rate of at least 150 s^{-1} was observed, again indicating that a step after chemical catalysis was partially rate limiting in the reverse reaction.

Kinetics of a Single Turnover. With the information in hand suggesting a rate-limiting step in the enzymatic reaction in each direction, we sought to examine more closely the events occurring at the enzyme site by conducting rapid quench experiments with enzyme in excess. In these experiments, the total conversion of radiolabeled substrate to product can be examined in a single turnover of the enzyme in order to directly observe events at the active site. In the first such experiment, excess enzyme (10 μM) was mixed with saturating S3P (100 μM) and limiting [^{14}C]PEP (3.5 μM), and the production of [^{14}C]EPSP was monitored. Under these conditions, the enzymatic reaction led to the formation of radiolabeled EPSP with the disappearance of PEP as shown in Figure 7. In addition, we saw the transient formation of pyruvate reaching a maximum at 10 ms corresponding to approximately 28% of the radiolabeled mixture and then decreasing to a level below detection limits at 100 ms. Control experiments established that neither EPSP nor PEP liberated pyruvate with the quenching conditions employed.

It is highly unlikely that the pyruvate itself is an intermediate in the reaction pathway, but rather, the pyruvate observed must be the breakdown product of an intermediate which is labile under acidic quench conditions. The time dependence of the formation and breakdown of this intermediate exactly parallels the disappearance of substrate (PEP) and the formation of product (EPSP) as fit by computer simulation of the time course. Therefore, there can be little question that the pyruvate is the breakdown product of a true intermediate in the reaction sequence.

We also looked for the appearance of the intermediate in the reverse direction by performing a single turnover experiment with enzyme in excess over EPSP and reacting with a high concentration of phosphate to drive the reaction in reverse. A solution of enzyme (10 μM) was mixed with a solution containing [^{14}C]EPSP (2.1 μM) and phosphate (7.5 mM). As

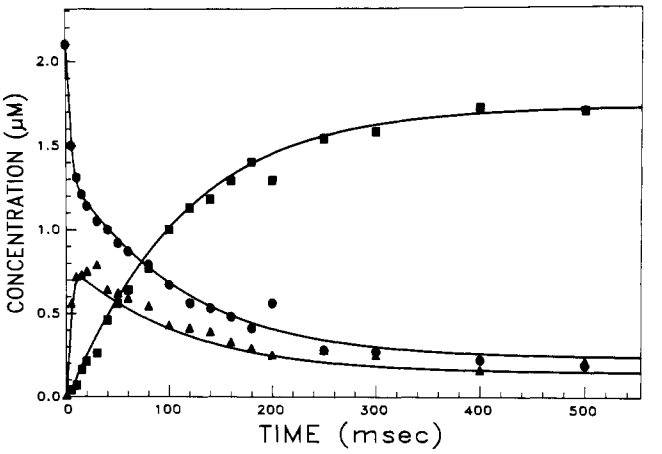

FIGURE 8: A single turnover in the reverse reaction. A solution of enzyme was mixed with a solution of [^{14}C]EPSP and phosphate. The final concentrations were enzyme (10 μM), [^{14}C]EPSP (2.1 μM), and phosphate (7.5 mM). The formation and disappearance of pyruvate (▲), EPSP (●), and PEP (■) were monitored. The curves were simulated by numerical integration with the rate constants summarized in Table II. Fitting the amplitudes of these curves required the additional constraint that phosphate binds to E·S3P complex with a dissociation constant of 0.67 mM.

shown in Figure 8, the transient formation and disappearance of pyruvate was noted along with the disappearance of substrate (EPSP) and formation of product (PEP). The enzyme intermediate reached a peak within 10–20 ms corresponding to 35% of the radiolabel in the mixture and then decreased to less than 7% after a period of 300 ms. As with the reaction in the forward direction, the transient appearance of pyruvate exactly paralleled the time dependence of product formation and decay of substrate.

A precise fit to the amplitude of the net reaction to produce PEP required us to include the weak binding of phosphate to the E·S3P complex (K_{d,P_i} = 0.67 mM) as shown in Table II. We confirmed that phosphate, at the high concentrations employed in this experiment, binds to enzyme in the presence of S3P by examining the competition with PEP in a single turnover experiment in the forward direction, analogous to the data described in Figure 7. The inhibition of the rate of the reaction of S3P to form the intermediate and EPSP supported quantitatively the postulated weak binding of phosphate to the E·S3P complex. In addition, Boocock and Coggins (1983)

Scheme III

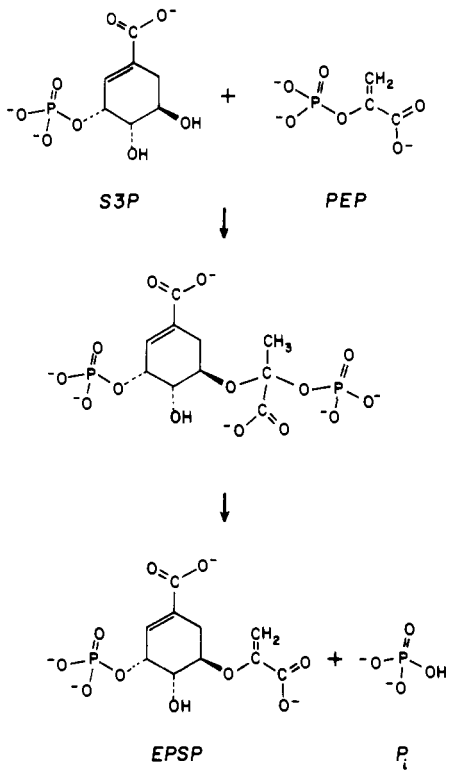

suggested the formation of an E·S3P·P_i complex to explain their steady-state kinetic data on the inhibition by glyphosate of the reverse reaction.

Nature of the Intermediate. The kinetics in the forward and reverse direction are indicative of a single intermediate in the reaction sequence (see Discussion). The simplest and most reasonable explanation is that the reaction proceeds by a direct addition–elimination reaction through a tetrahedral intermediate as shown in Scheme III. The breakdown of this intermediate in acid to produce S3P and pyruvate can be rationalized as described under Discussion. Moreover, this analysis predicts that a different distribution of products should be obtained from the breakdown of the intermediate at high pH. Therefore, to further explore the nature of this intermediate, we conducted a quench experiment in the presence of base.

A single turnover experiment in the forward reaction analogous to the one described in Figure 7 was conducted except the reaction was quenched with base (0.6 M KOH followed by chloroform and neutralization) and a higher enzyme concentration was used (40 μM) to produce more of the intermediate in the first 10 ms of the reaction. The distribution of label from [^{14}C]PEP into pyruvate, PEP, and EPSP was then determined by HPLC. As summarized in Table I, upon quenching under basic conditions, compared to an identical experiment quenched with acid, there was less pyruvate formed, but more PEP and EPSP. The data shown were obtained by quenching after 10 ms of reaction, corresponding to the peak in pyruvate production; a similar partitioning was observed over the time interval from 5 to 25 ms where pyruvate could be detected indicating that there was no time-dependent change in the partitioning of the intermediate into the three breakdown products.

These data provide strong support for a tetrahedral intermediate as shown in Scheme III. If one assumes 100% conversion of the intermediate to pyruvate in the acid quench, then in the base quench 30% of the intermediate breaks down to form PEP while 40% of the intermediate yields EPSP (Table I). This implies that the all of the chemical entities present in both PEP and EPSP are constituents of the intermediate. The tetrahedral intermediate shown in Scheme III is the most reasonable structure to account for these data.

An alternate suggestion for an enzyme intermediate involves a covalent enzyme–enolpyruvoyl adduct (Anton et al., 1983). This intermediate has been suggested in order to account for the incorporation of tritium from solvent into PEP in the presence of 4,5-dideoxyshikimic acid 3-phosphate (dideoxy-S3P), an analogue which lacks the 5-OH group necessary for chemical reaction. The tetrahedral intermediate shown in Scheme III could not form from the dideoxy-S3P, and therefore, our mechanism, in its simplest form, would not predict tritium exchange into PEP in the presence of dideoxy-S3P. However, if the enzyme were going through a covalent enzyme–enolpyruvoyl intermediate as suggested by Anton et al., pyruvate should be liberated upon quenching with acid after incubation of the enzyme with dideoxy-S3P and PEP. In order to test this hypothesis, a high concentration of enzyme (200 μM) was incubated with dideoxy-S3P (5 mM) and [^{14}C]PEP (10 μM). These concentrations were chosen to saturate the enzyme with dideoxy-S3P and for 90% of the PEP to be bound to the enzyme (in large excess) according to the measured dissociation constants determined by fluorescence titrations as described under Materials and Methods. The values obtained for the dissociation constants were 100 μM for dideoxy-S3P binding to enzyme and 23 μM for PEP binding to the E·didexoy-S3P complex. Upon quenching the E·dideoxy-S3P·PEP* complex with acid, there was no pyruvate obsrved within the detection limits of ~0.5%, and all of the label was recovered as PEP. This observation supports the mechanism shown in Scheme III.

In the reverse reaction, it might be postulated that EPSP first reacts with the enzyme to form a covalent enzyme–enolpyruvoyl intermediate, which then reacts with phosphate to form PEP. To examine this possibility, a single turnover experiment was conducted by mixing an excess of enzyme with [^{14}C]EPSP as described in Figure 8, but in the absence of phosphate, and then quenching with acid. Although EPSP is hydrolyzed by the enzyme at a slow rate in the absence of phosphate (4.7×10^{-4} s^{-1}), no pyruvate was produced after quenching on a time scale which is relevant to catalysis. Within the limits of detection of 0.5%, these data argue that the intermediate we observed is not formed in the absence of phosphate, supporting the identification of the tetrahedral intermediate. However, in this case, substrate synergism involving phosphate binding energy to activate the EPSP toward reaction with an enzyme nucleophile cannot be ruled out.

The Chemical Equilibrium Constants. The overall solution equilibrium constant and the internal equilibrium constant at the active site of the enzyme were measured directly by separation and analysis of radiolabeled products and reactants formed under different equilibrium conditions.

The overall solution equilibrium constant was determined by mixing [^{14}C]EPSP (doubly labeled; 4 μM) and phosphate (1 mM) with a low concentration of enzyme (0.1 μM) and allowing the mixture to come to equilibrium (3 h). Simulation of the reaction time course and analysis of the reaction mixture at various times after mixing confirmed that equilibrium had been attained. The sample was quenched with acid and neutralized, and the relative distributions of radiolabeled S3P, PEP, and EPSP were determined. The equilibrium constant was calculated from the ratio

$$K_{eq} = [EPSP][P_i]/[S3P][PEP] = 180$$

The enzymatic reaction was energetically favorable in the forward direction with a net free energy change, $\Delta G^\circ = -3.0$ kcal/mol.

The internal equilibrium constant was determined by incubating [^{14}C]S3P (4 μM), with high concentrations of PEP (2 mM), and phosphate (10 mM) and a high concentration of enzyme (16 μM) so that all radiolabeled products would be bound to the enzyme. The sample was quenched with acid after 5–10-s incubation and then neutralized, and the distribution of label between EPSP and S3P was determined. The data provided a ratio of [EPSP]/[S3P] = 2.3. In the simplest interpretation, this number would provide the equilibrium constant between the enzyme forms, E·S3P·PEP $\rightleftarrows$ E·EPSP·P_i. However, because the intermediate breaks down upon acid quench to liberate S3P, the complete internal equilibrium must be considered:

$$\text{E·S3P·PEP} \underset{k_{-3}}{\overset{k_3}{\rightleftharpoons}} \text{E·I} \underset{k_{-4}}{\overset{k_4}{\rightleftharpoons}} \text{E·EPSP·P}_i$$

Accordingly, the apparent equilibrium constant measured gives the ratio

$$K_{int}^{app} = \frac{[\text{E·EPSP·P}_i]}{[\text{E·S3P·PEP}] + [\text{E·I}]}$$

Complete analysis of the time course of the kinetics of formation and breakdown of the intermediate in the forward and reverse reactions require that the equilibrium constant K_3 is large; and so, the measured ratio is $K_{int}^{app} \simeq K_4 = [\text{E·EPSP·P}_i]/[\text{E·I}] \simeq 2.3$.

The simulated curves in Figures 1–8 were generated from the same set of 12 rate constants (Table II) with the KINSIM enzyme kinetics simulation program. In addition to the solution and internal equilibrium constants, the rate constants for the reaction were further constrained by dissociation constants and binding rates for S3P and EPSP previously determined (Anderson et al., 1988a) as well as previously reported K_m values for substrates (Duncan et al., 1984).

Discussion

In this paper we have provided a direct demonstration of an intermediate in the reaction catalyzed by EPSP synthase. The time dependence of formation of pyruvate in the rapid quench follows exactly the kinetics predicted for an intermediate. The intermediate is kinetically competent in that it is formed and broken down at a rate sufficient to account for catalytic turnover. In both the forward and the reverse reactions the intermediate rises rapidly in a reaction which parallels the loss of substrate and then decreases as the product is formed. The simulation of the kinetics demonstrates that the reaction can be fit precisely with the formation and breakdown of a *single kinetic intermediate* in the reaction pathway between substrate and product.

A True Kinetic Intermediate. The kinetics demonstrating the formation of this intermediate are unequivocal. One set of rate constants has been obtained which can account for every kinetic trace described in this paper including reactions in the forward and the reverse direction, with enzyme in excess or with substrate in excess, and with experiments designed to measure internal and overall equilibria. In addition, experiments not shown were conducted at different enzyme concentrations or substrate concentrations and again can be accounted for by the set of rate constants which have been selected. The uniqueness of this set of rate constants depends to large extent upon the constraints which have been placed upon them by our knowledge of the binding constants for S3P and EPSP, by the Michaelis constants for PEP and phosphate, and by our measurement of the internal equilibrium constant and the overall equilibrium constant. The fitting of the data in the simulation process has been refined in its final stages by error analysis examining the sum square error with respect to each parameter and allowing minimization.

On the basis of these kinetic parameters (Table II), we now understand why only a partial burst amplitude was observed in Figures 5 and 6 examining the pre-steady-state transient with substrate in excess. Product release is only partially rate limiting in each direction. In the forward reacton, phosphate release is primarily rate limiting, but the products are involved in an internal equilibrium to form the intermediate thereby reducing the steady-state concentration of products bound to the enzyme. In the reverse reaction, the breakdown of the intermediate is the predominant rate-limiting step, but the internal equilibrium favors the formation of EPSP, thus lowering the burst amplitude.

Kinetics of Substrate Trapping. The substrate trapping experiments establish relatively fast dissociation rates for both S3P and EPSP. Combined with the measured equilibrium dissociation constants, these data imply that the substrates bind in a rapid equilibrium manner, and therefore, their dissociation constants are approximately equal to their Michaelis constants. S3P and EPSP, in particular, bind and dissociate in very rapid reactions. The binding rate of S3P, 6.5×10^8 M^{-1} s^{-1}, is among the fastest second-order rate constant measured for substrate binding to an enzyme and implies that the binding is diffusion limited. In the forward reaction, rapid equilibrium binding of S3P is followed by the rate-limiting binding of PEP which then leads to the formation of the enzyme-bound intermediate.

The basis for trapping less than 100% of the S3P at saturating PEP (Figure 2) is subject to some speculation. Several possible explanations can be considered: (1) There may be a fraction of enzyme (30%) which is inactive, leading to a lower concentration of E·S3P than expected; however, we minimized errors due to dead protein by determining the enzyme concentration by active site fluorescence titration with S3P and glyphosate (Anderson et al., 1988a) and by performing the trapping experiment with enzyme in excess. (2) The dissociation constant for S3P could be underestimated; however, the K_d was determined by three independent measurements to be 7–8 μM (Anderson et al., 1988a), and a value of 30 μM would be needed to account for the data. (3) S3P may dissociate from the ternary E·S3P·PEP complex; however, the experiment designed to measure the internal equilibrium constant demonstrated that a high concentration of PEP can prevent S3P from dissociating from the enzyme. Moreover, the rate of dissociation required to account for 70% trapping (300–600 s^{-1}) is faster than the rate-limiting PEP release (k_{-2}) determined from the pre-steady-state kinetics in the reverse direction. (4) It is conceivable that 30% of the S3P binds to the enzyme in a mode that is not productive for catalysis. There is little rigorous data to support nonproductive binding, and the chemical meaning is not entirely clear; nonetheless, this remains as the only feasible explanation of the 70% trapping efficiency.

Free Energy Profile. The reaction free energy coordinate for this enzyme-catalyzed mechanism is shown in Figure 9. With a reaction of this type, having only a small overall external equilibrium constant (180), it is important for efficient catalysis that no one step in the reaction has a large change in free energy. Otherwise, the enzyme would fall into a deep thermodynamic well. The internal equilibrium, involving the

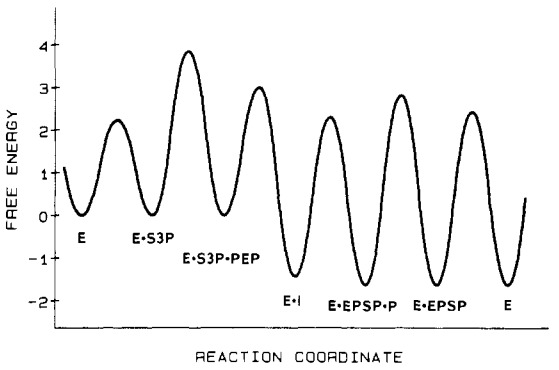

FIGURE 9: Reaction free energy profile for EPSP synthase. The free energy change and the apparent free energies of activation for each step of the reaction were calculated from the constants given in Table II for the reaction in the forward direction as shown in Scheme II. The concentrations of substrates and products were set equal to their dissociation constants: [S3P] = 7 μM, [PEP] = 18 μM, [EPSP] = 1 μM, and [P_i] = 1.43 mM, concentrations which are thought to approximate the physiological conditions. The relative apparent free energies of activation were calculated as $\Delta G^* = RT[\ln (k_B T/h) - \ln (k_{obsd})] - 10$ kcal/mol, where k_B is the Boltzmann constant. The value of 10 kcal/mol was arbitrarily chosen to be subtracted from the values calculated so that the relative magnitudes of the activation energies could be better illustrated in this graph.

reaction of S3P and PEP to form EPSP and P_i, occurs in two steps ($K_3K_4 = 17$) accounting for half of the standard-state free energy change for the reaction in solution and perhaps nearly all of the free energy change under physiological conditions. The largest free energy change occurs with the formation of the intermediate.

One can calculate the enzymatic efficiency as the ratio of the enzymatic flux to the diffusion-limited rate of collision of the substrate with the enzyme operating reversibly under physiological conditions (Albery & Knowles, 1976). Assuming that $k_1 = 6.5 \times 10^8$ M^{-1} s^{-1} represents the diffusion-limited rate of collision for S3P and that the physiological concentration of S3P equals the dissociation constant, we calculate an efficiency function of 0.006. A similar calculation yields an efficiency of 0.025 for EPSP in the reverse reaction. Comparable or smaller efficiencies are calculated for PEP and phosphate, depending upon the value chosen for the diffusion-limited rate of collision. In each case this enzymatic efficiency function, defined as the number of chemical conversions per collision event, is small because the substrates come to equilibrium in binding to the enzyme during turnover at physiological concentrations.

Nature of the Intermediate. The identity of the enzyme intermediate has not been proven but can be inferred by chemical and kinetic arguments. Evidence for the intermediate was obtained as the transient appearance of pyruvate due to the breakdown of the presumed intermediate in the acid quench. The production of pyruvate from the breakdown of the intermediate can be seen only when experiments were conducted with radiolabel in the PEP or in the carboxyvinyl portion of EPSP, because the other breakdown products are S3P and phosphate, normal reactants in the enzymatic pathway.

The kinetics of the reaction require that there be a single kinetic intermediate. However, as with any kinetic mechanism, one can always insert an additional step so long as it is fast enough in both directions such that it is never observed. For example, it has been postulated that a covalent enol-pyruvoyl–enzyme intermediate is formed from PEP and then reacts with S3P. To account for the kinetics, the enzyme-bound nucleophile would have to be very reactive in both the

Scheme IV

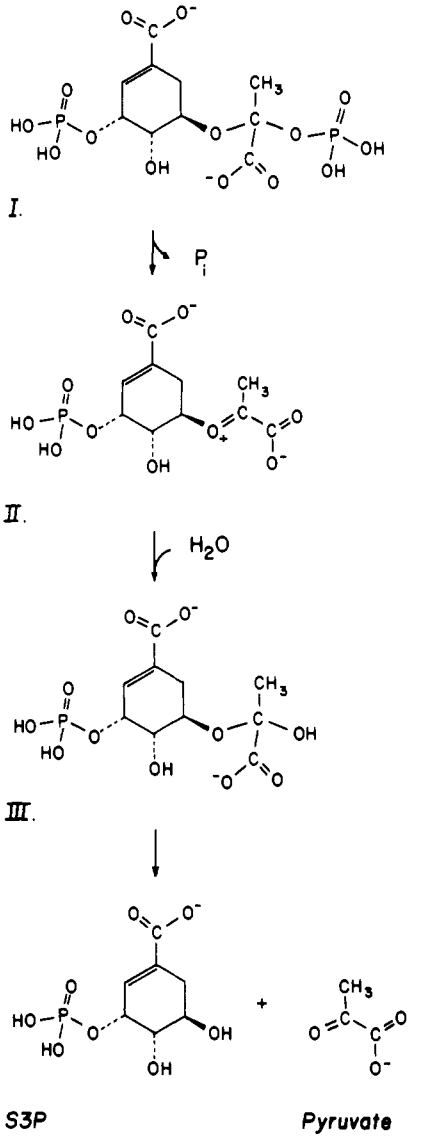

forward and reverse directions such that it never accumulated and never affected the observed kinetics. However, in the absence of any solid evidence in favor of such an additional intermediate, a simpler mechanism must prevail.

Our data support a direct addition–elimination mechanism involving a nucleophilic attack of the 5-OH directly on the C-2 of PEP leading to the formation of a tetrahedral intermediate as shown in Scheme III. The breakdown of the tetrahedral intermediate under acidic conditions can be rationalized as shown in Scheme IV. When the intermediate (I) is subjected to strongly acidic conditions, the phosphate group becomes protonated, facilitating its loss, perhaps via the formation of an oxonium (II) species as shown in Scheme IV. The addition of H_2O to this species would give an unstable hemiketal (III) which would breakdown to yield S3P and pyruvate. A similar mode of acid hydrolysis has been suggested for α-D-glucose 1-phosphate (Bunton et al., 1958).

Stereoelectronic theory predicts that breakdown of this tetrahedral intermediate (I) is facilitated by the nonbonded electron pairs on the oxygen atoms bonded directly to the tetrahedral carbon, with a thermodynamic preference for loss of the group oriented antiperiplanar to the lone electron pair (Deslongchamps, 1983; Gorenstein, 1987). Accordingly, the intermediate could break down with loss of either S3P or P_i. At low pH, loss of P_i is preferred, followed by hydrolysis to

yield pyruvate and S3P as described above. Under strongly basic conditions, removal of a proton from the methyl group would lead to production of EPSP following the loss of P_i or to the recovery of PEP following the loss of S3P.

The data shown in Table I demonstrate that the breakdown of the tetrahedral intermediate is indeed a function of pH. At high pH the intermediate partitions to yield pyruvate (30%), PEP (30%), and EPSP (40%). The important conclusion from these data is that the intermediate must contain moieties donated by both PEP and EPSP. The tetrahedral structure (Scheme IV, I) shown is the only logical reaction intermediate. Moreover, the predicted pH-dependent breakdown of the tetrahedral intermediate is consistent with our data.

It is unexpected, perhaps, that the proposed tetrahedral intermediate would be unstable under basic conditions because the base-catalyzed elimination involving the loss of a proton from the C-3 methyl group would be unfavorable. It has been reported that a derivative of neuraminic acid, *N*-acetyl-β-D-neuraminic acid 2-phosphate, can be isolated under mildly basic conditions (Beau et al., 1984). This compound contains similar functional groups as those in the proposed tetrahedral intermediate. On the basis of this precedent, we have sought and found conditions under which the intermediate is stable and can be isolated from the enzyme. Spectroscopic evidence supports our structural assignment of the tetrahedral intermediate (Anderson et al., 1988b). Further work is in progress to fully characterize the intermediate and to measure the pH dependence of its breakdown.

The only evidence in favor of a covalent enolpyruvoyl–enzyme intermediate was that provided by Anton et al. (1983). They reported a slow rate of tritium exchange of the methylene protons of PEP upon incubation of enzyme with dideoxy-S3P. In our experiments, we have looked for the appearance of pyruvate following mixing of the enzyme with dideoxy-S3P and radiolabeled PEP at concentrations sufficient to saturate the enzyme site. There was no pyruvate formed following this incubation, providing support for our model.

In looking for the postulated enolpyruvoyl–enzyme intermediate, we carefully designed conditions to saturate the enzyme with dideoxy-S3P and PEP with enzyme in excess over the PEP. If an enzyme–enolpyruvoyl intermediate were formed, one might expect to see more of the intermediate accumulating in this experiment than we observed transiently in the presence of the reactive 5-OH group of the S3P. Accordingly, the failure to see any pyruvate following acid quenching of the enzyme incubated with dideoxy-S3P and PEP further weakens the arguments suggesting a covalent enolpyruvoyl intermediate.

One might argue that the failure to observe pyruvate and the extremely slow rate of exchange observed by Anton et al. might be due to substrate synergism, postulating that the 5-OH of S3P is necessary to provide sufficient binding energy for PEP to become activated to react against the enzyme nucleophile to form the enolpyruvoyl–enzyme intermediate. Dideoxy-S3P binds only 14-fold weaker than S3P, and the binding constant for PEP in the presence of dideoxy-S3P is comparable to that in the presence of S3P. It is therefore difficult to reconcile this quantitative binding data with a rate of tritium incorporation in the presence of dideoxy-S3P which was 300-fold slower than turnover (Anton et al., 1983).

The slow tritium exchange observed by Anton et al. could be reconciled with our mechanism if the protonation of the methylene group of PEP led to the formation of a carbonium ion at the enzyme active site. This process would be greatly facilitated due to the proximity of the 5-OH group and lead to the formation of the tetrahedral intermediate with the normal substrate. When the 5-OH is missing, the carbonium ion may be sufficiently stabilized, perhaps by a base at the active site, to account for the slow rate of exchange observed with dideoxy-S3P.

The only other enzyme known to carry out this type of chemistry using phosphoenolpyruvate to donate an enolpyruvoyl group is UDP-enolpyruvoyl transferase (Zemell & Anwar, 1975). With this enzyme, there is some evidence for an enolpyruvoyl enzyme intermediate. Incubation of the enzyme with [^{14}C]PEP led to incorporation of counts into the protein although the reaction was not well characterized. This precedent of an enzyme-bound enolpyruvoyl intermediate, more than any real data on EPSP synthase, has provided the impetus to suggest a covalent intermediate with EPSP synthase.

Glyphosate Binding. Only EPSP synthase is inhibited by the herbicide glyphosate, which competes with PEP in binding to the enzyme in the presence of S3P (Steinrucken & Amrhein, 1980). The data presented in this paper pose the interesting suggestion that glyphosate binds with S3P at the active site so as to mimic the binding of the terahedral intermediate to the enzyme. For example, it is reasonable to suppose that the amino group of glyphosate is positioned to accept a hydrogen bond from the group which donates a proton to the methylene group of PEP. The quantitative data presented in this paper and our previous work (Anderson et al., 1988a) allow for a thermodynamic and kinetic comparison between PEP and glyphosate. Glyphosate binds to E·S3P 115-fold tighter (18.5 μM/0.16 μM) and 20-fold slower (15 μM^{-1} s^{-1}/0.78 μM^{-1} s^{-1}) than PEP, while the rate of dissociation of glyphosate is 2300-fold slower than that of PEP (280 s^{-1}/0.12 s^{-1}) (Table II). It is pointless to argue whether glyphosate is a transition-state or a ground-state analogue; certainly, if glyphosate were a perfect ground-state analogue, it would bind with kinetic and thermodynamic constants identical with those of PEP. The more reasonable approach is to suggest that the S3P–glyphosate complex interacts favorably with groups at the active site that normally serve to stabilize the tetrahedral intermediate. Moreover, our data predict that an analogue of the tetrahedral intermediate would be a potent inhibitor of the enzyme.

ACKNOWLEDGMENTS

We thank Dr. Michael J. Miller for the synthesis and purification of the dideoxy-S3P used in this study. We also thank Dr. William P. Jencks for a thorough reading of the manuscript and for the suggestion that the tetrahedral intermediate should be stable at higher pH.

REFERENCES

Albery, W. J., & Knowles, J. R. (1976) *Biochemistry 15*, 5631–5640.

Anderson, K. S., Sikorski, J. A., & Johnson, K. A. (1988a) *Biochemistry 27*, 1604–1610.

Anderson, K. S., Sikorski, J. A., Benesi, A. J., & Johnson, K. A. (1988b) *J. Am. Chem. Soc. 110*, 6577–6579.

Anton, D. L., Hedstrom, L., Fish, S. M., & Abeles, R. H. (1983) *Biochemistry 22*, 5903–5908.

Barshop, B. A., Wrenn, R. F., & Frieden, C. (1983) *Anal. Biochem. 130*, 134–145.

Beau, J.-M., Schauer, R., Haverkamp, J., Kamerling, J., Dorland, L., & Vliegenthart, J. (1984) *Eur. J. Biochem. 140*, 203–208.

Bondinell, W. E., Vnek, J., Knowles, P. F., Sprecher, M., & Sprinson, D. B. (1971) *J. Biol. Chem. 246*, 6191–6196.

Boocock, M., & Coggins, J. (1983) *FEBS Lett. 154*, 127-132.
Bunton, C. A., Llewellyn, D. R., Oldham, K. G., & Vernon, C. A. (1958) *J. Chem. Soc.*, 3588-3594.
Deslongchamps, P. (1983) *Stereoelectronic Effects in Organic Chemistry*, Pergamon, Oxford, U.K.
Duncan, K., Lewendon, A., & Coggins, J. R. (1984) *FEBS Lett. 165*, 121-127.
Gorenstein, D. G. (1987) *Chem. Rev. 87*, 1047-1077.
Grimshaw, C. E., Sogo, S. G., & Knowles, J. R. (1982) *J. Biol. Chem. 257*, 596-598.
Hammond, G. S. (1955) *J. Am. Chem. Soc. 77*, 334.
Johnson, K. (1986) *Methods Enzymol. 134*, 677-705.
Lanzetta, P., Aflvarez, L. J., Reinach, P. S., & Candia, O. A. (1979) *Anal. Biochem. 100*, 95-97.
Millar, G., Lewendon, A., Hunter, M. G., & Coggins, J. R. (1986) *Eur. J. Biochem. 237*, 427-437.
Pittard, J., & Ely, B. (1979) *J. Bacteriol. 138*, 933-943.
Rogers, S. G., Brand, L. A., Holder, F. B., Sharps, E. S., & Brackin, M. J. (1983) *Appl. Environ. Microbiol. 46*, 37-43.
Rose, I. A. (1980) *Methods Enzymol. 64*, 47-59.
Steinrucken, H. C., & Amrhein, N. (1980) *Biochem. Biophys. Res. Commun. 94*, 1207-1212.
Steinrucken, H. C., & Amrhein, N. (1984) *Eur. J. Biochem. 143*, 341-357.
Zemell, R. I., & Anwar, R. A. (1975) *J. Biol. Chem. 250*, 4959-4964.

Preparation and Reconstitution with Divalent Metal Ions of Class I and Class II *Clostridium histolyticum* Apocollagenases†

Eddie L. Angleton and Harold E. Van Wart*
Department of Chemistry and Institute of Molecular Biophysics, Florida State University, Tallahassee, Florida 32306
Received February 26, 1988; Revised Manuscript Received May 23, 1988

ABSTRACT: Both γ- and ζ-collagenases from *Clostridium histolyticum* are fully and reversibly inhibited by 1,10-phenanthroline at pH 7.5 in the presence of 10 mM $CaCl_2$ with K_I values of 0.11 and 0.040 mM, respectively. The inhibition is caused by removal of the single, active-site Zn(II) present in each of these enzymes. The nonchelating analogue 1,5-phenanthroline has no effect on the activity of either enzyme. Dialysis of the enzymes in the presence of 1,10-phenanthroline, followed by back dialysis against buffer containing no chelating agent, gives the respective apocollagenases. Both apoenzymes can be instantaneously and fully reactivated by the addition of 1 equiv of Zn(II). Variable amounts of activity are restored to both apocollagenases by Co(II) and Ni(II) and to γ-apocollagenase by Cu(II). The activity titration curve for γ-apocollagenase with Co(II) and Scatchard plots for the reconstitution of γ-apocollagenase with Cu(II) and Ni(II) and of ζ-apocollagenase with Ni(II) and Co(II) indicate that all activity changes are the result of binding of a single equivalent of these divalent metal ions at the active site of the collagenases. Cd(II) and Hg(II) do not restore measurable activity to either apoenzyme.

The culture filtrate of *Clostridium histolyticum* contains at least seven distinct collagenases (EC 3.4.24.3)[1] with molecular weights that vary from 68000 to 130000 (Bond & Van Wart, 1984a,b). These enzymes have been divided into two classes that differ with respect to their sequences, as determined by chromatographic analysis of their tryptic digests and cyanogen bromide reaction products (Bond & Van Wart, 1984c), their mode of attack on native collagen (French et al., 1987), their relative activities toward synthetic peptides (Steinbrink et al., 1985; Van Wart & Steinbrink, 1985; Mookhtiar et al., 1985), and their differential inhibition by substrate analogues (Mookhtiar et al., 1988). Early studies showed that these collagenases are reversibly inhibited by chelating agents and led to the suggestion that they are metalloproteinases (Seifter & Harper, 1971). Confirmation of this has been provided by direct metal determination using atomic absorption spectroscopy which has demonstrated that these collagenases contain 1 mol of zinc/mol of protein and variable amounts of calcium ions (Bond & Van Wart, 1984b). Both the zinc and calcium ions are required for activity (Bond et al., 1981). The zinc ion is believed to be present at the active site, and the calcium ions are believed to stabilize the tertiary structure of the protein, as observed for thermolysin (Latt et al., 1969; Feder et al., 1971).

Since these collagenases contain an active-site zinc ion as an intrinsic, functional constituent, it is of interest to examine the role of the zinc ion in catalysis. Studies of the effects of active-site metal substitutions on the activities of zinc metalloenzymes have historically been a fruitful means of exploring the functional role of zinc (Vallee & Galdes, 1984). In this study, the mechanism of inhibition of a representative class I (γ) and class II (ζ) collagenase by the transition metal chelating agent 1,10-phenanthroline has been investigated, and the respective apocollagenases have been prepared. These species have been reconstituted with various divalent metal ions, and the effects on peptidase activity have been measured. This represents the first intensive investigation of the role of the active-site metal ion for any collagenase and lays the basis for examining the kinetic properties of the resulting metallocollagenases in more detail (Angleton & Van Wart, 1988).

† Supported by National Institutes of Health Research Grant GM27939 and Research Career Development Award AM01066 (to H.E.V.W.).
* Author to whom correspondence should be addressed.

[1] Abbreviations: Hepes, *N*-(2-hydroxyethyl)piperazine-*N*′-ethanesulfonic acid; FALGPA, 2-furanacryloyl-L-leucylglycyl-L-prolyl-L-alanine; *Clostridium histolyticum* collagenase is referred to as collagenase; the various metallocollagenases are designated [(CHC)M(II)], where the brackets denote the firm binding of the divalent transition metal ion, M(II), to the apoenzyme, CHC.

0006-2960/88/0427-7406$01.50/0